TRIUMF Beam Physics Note
TRI-BN-25-01
January 13, 2025

Beamline 1A Collimator Optimization

Lige Zhang

TRIUMF

Abstract: This note describes the optimization of the collimators after T2 target, covering the geometry parameters and performance specifications in sufficient details for proceeding to the mechanical/engineering design.

1 Introduction

The collimator following the T2 target is designed to remove the scattering halo from the 480 MeV proton beam passing through the T2 target. Beam losses downstream of the collimator, but upstream of the TNF target, must be minimized to protect critical components such as quadrupoles and diagnostics and to reduce activation. At the same time, achieving high transmission through the collimation section is essential to minimize the heat load on the collimator and to maximize the yield at the TNF target.

2 Requirements and Constraints

2.1 General requirement

The collimator must fit within the space between the T2 exit and the Q14 entrance. The geometric envelope of the available space is determined by the current collimator geometry.

The collimator should be designed to localize beam spills in coordination with the three scraper boxes positioned between T2 and TNF, thereby minimizing the shielding requirements.

It is crucial to minimize beam losses on beamline elements between T2 and TNF, especially on the quadrupoles located immediately downstream of the collimator.

Additionally, the design should aim to maximize beam transmission to reduce heat dissipation on the collimator and enhance the yield at the TNF target station.

2.2 Specific Requirements

The T2 Beryllium target may possess diffrerent lengths, e.g. 0, 12 mm, 50mm or 100 mm, depending on the user's requirement. These cases have been simulated with G4beamline[1, 2], concerning the issues of Coulomb scattering, energy loss and energy loss straggling. In brief, for dffrerent thicknesses of T2 target, the collimator should have different optimal aperture. As per Syd Kreitzman's advice, the conceptual design work can commence using 5 cm Be targets.

Normal beam size (2rms) on the target is is 2-3 mm horizontally and 6- 7 mm vertically. The thermal calculations indicate that targets should survive proton beam currents of 150 μA with the normal beam spot.[3]

3 Optics and beam losses

The layout of the components is shown in the upper plot in Fig. 3. The magenta cylinders represent the collimators, while the green ones are the quads. Following the triplet, there are three scraper boxes; the first scraper is shorter, designed to minimize back scattered neutrons.

The beamline model used in this note to optimize the collimator is built and refined from Fred's original BL1A g4beamline model [4]. The g4beamline model is compared with TRANSOPTR model [5], shown in Fig. 1. The beam envelopes from these 2 models agree with each other.

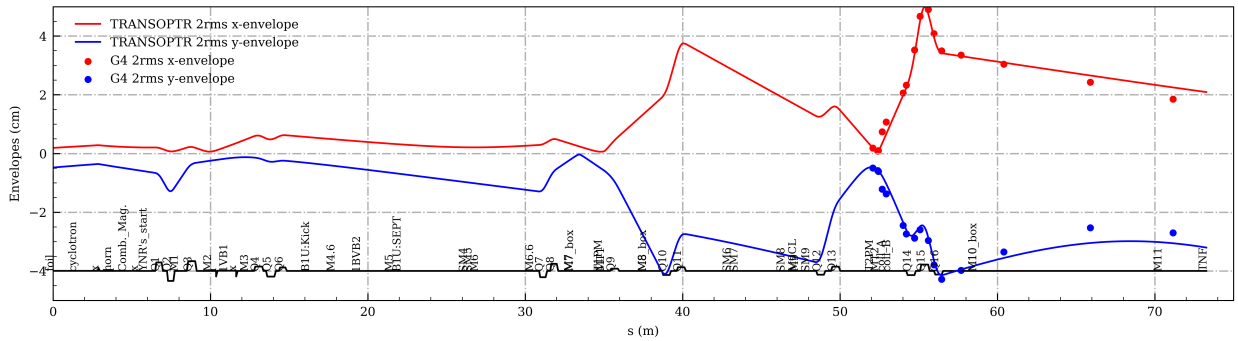

Figure 1: Beam envelopes calculated using TRANSOPTR and G4Beamline. The G4 simulation model starts from T2 protection Monitor, and the initial beam distribution is Gaussian with the sigma matrix parameters obtained from TRANSOPTR. In this note, T2 is default a 5 cm Be target in the simulation. The discrepancy in the envelopes arises from the non-Gaussian distribution after the beam passes through the T2 target and the lack of collimator in TRANSOPTR model. The difference between the two simulation models is within 15% along the beam line.

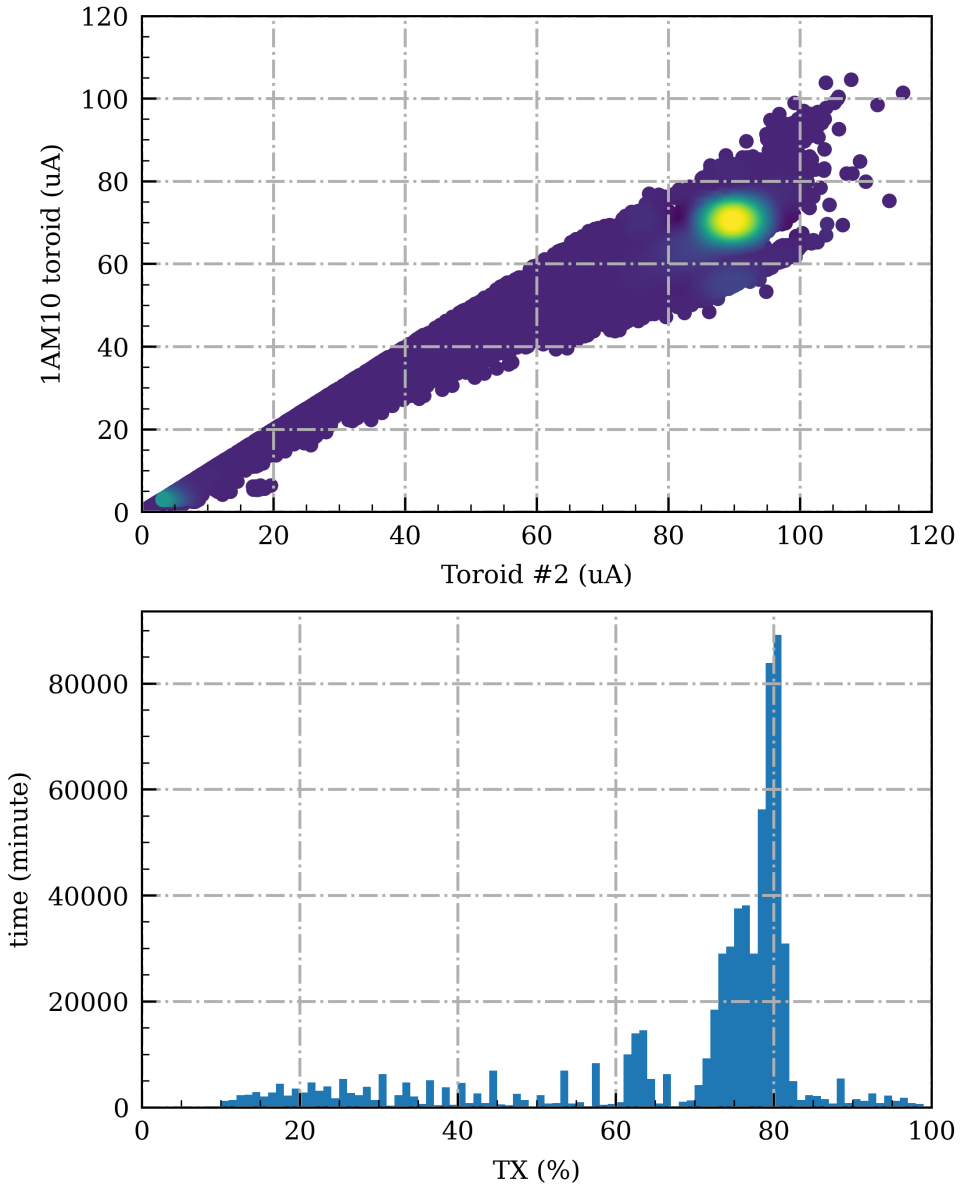

Figure 2: Transmission of the collimation section under production run in the past 3 years. Toroid #2 is a non-intercepting diagnostic device used to measure the beam current before the T2 target. Similarly, 1AM10 measures the beam current after the T2 collimation section. In the upper plot, brighter colors indicate longer production times at the corresponding intensity levels. The transmission of the collimation section is derived from the slope of 1AM10 vs. Toroid #2, as summarized statistically in the lower plot.

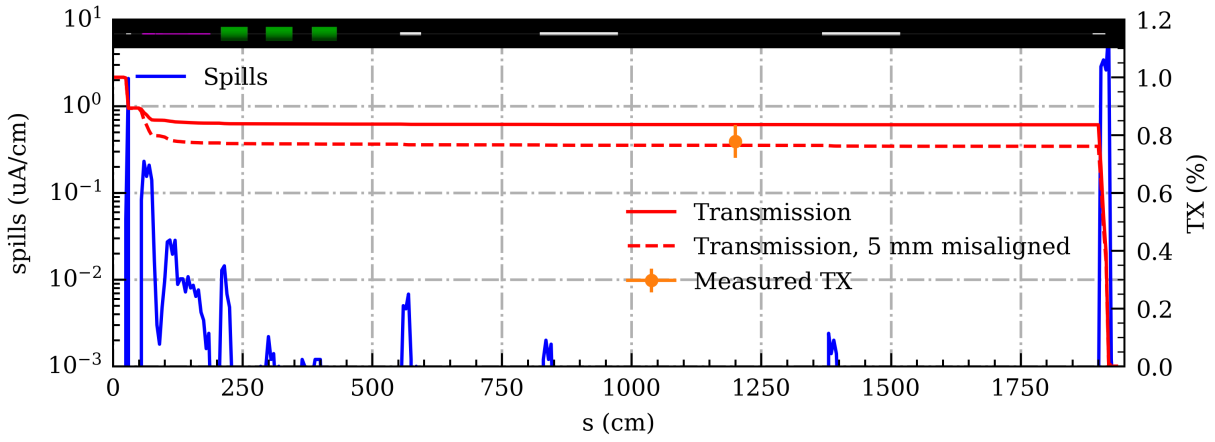

Figure 3: Layout of the components and beam spills along the beamline between T2 and TNF. The beam loss rate on the T2 target is approximately 2 uA/cm with a primary beam intensity of 100 uA, resulting from non-elastic nuclear reactions. The second peak, at around 0.2 uA/cm, represents the collimated beam on COL A. The loss rate on COL B is ten times smaller than A. In the post-collimation section, the maximum loss rate is approximately 0.02 uA/cm, occurring at Q14, the first quads following the collimator. Beam loss downstream of the triplet is confined to the scraper box, with a loss rate of less than 0.01 uA/cm. The discrepancy between measured and calculated transmission could be explained by collimator misalignment. With a typical vertical alignment error of 5 mm, the calculated transmission drop in the collimator section is doubled.

3.1 Beam losses

The transmission of the collimation section under BL1A production runs over the past three years is shown in Fig. 2. These values are calculated based on beam intensity measurements taken before and after the T2 section during this period. Beam losses between T2 and TNF were simulated using the G4beamline model, with the results presented in Fig. 3 and compared to the measured transmission data. The heat load on the collimators caused by beam losses was also calculated and compared to cooling system readings, as summarized in Table 1.

Table 1: Collimator cooling parameters with 112.8 uA on T2.

Collimator	**Inlet (°C)**	**Outlet (°C)**	**Flow rate (gpm)**	**Cooling power (W)**	**Simulated heat load (W)**
A	22.9	27.8	1.3	1243.0	1868.7
B	22.9	27.6	0.7	643.3	544.8

3.2 Beam Scattering on the T2 Target

The 70-500 MeV proton beam with a pure Gaussian approximation leads to the Highland-Lynch-Dahl equation 1 to describe the scattering angle θ_{sc}

$$\theta_{\rm sc} = \frac{13.6\,{\rm MeV}}{\beta cp}\sqrt{\frac{x}{X_0}}\left[1 + 0.038\ln\left(\frac{x}{X_0}\right)\right] \tag{1}$$

Where X_0 is the radiation length, E is the beam energy, z is the travelling distance in the material of the beam. Under the condition of $10^{-}3 < z/X_0 < 100$, this equation is accurate to 11% or better. With small energy loss in the target, E could be treated as a constant in Eq.(1).

The multi-scattering angle of a 475 MeV proton beam passing through 5 cm of beryllium is 10.6 mrad (2rms).

In a Gaussian approximation, the divergence angle of the beam after passing through the target is given by $\sqrt{\theta_{sc}^2 + \theta_0^2}$. In our beamline, the divergent angle of the beam before passing through the target is 6.2 mrad (2rms) horizontally and 7.5 mrad (2rms) vertically. Consequently, after the T2 target, the angular envelope increases by approximately a factor of 2. As shown in Fig. 18. After scattering, the 4 RMS of the beam remains within the vacuum pipe. However, the slowly decreasing tails of the single scattering distribution result in a beam intensity outside the 4 RMS that is significantly larger than a Gaussian beam. Therefore, a collimator should be placed downstream of T2 to remove the halo that could potentially strike the pipe between T2 and TNF. The envelope of the halo that could hit the pipe is calculated based on the existing triplet optics and the proposed double doublets optics model [6].

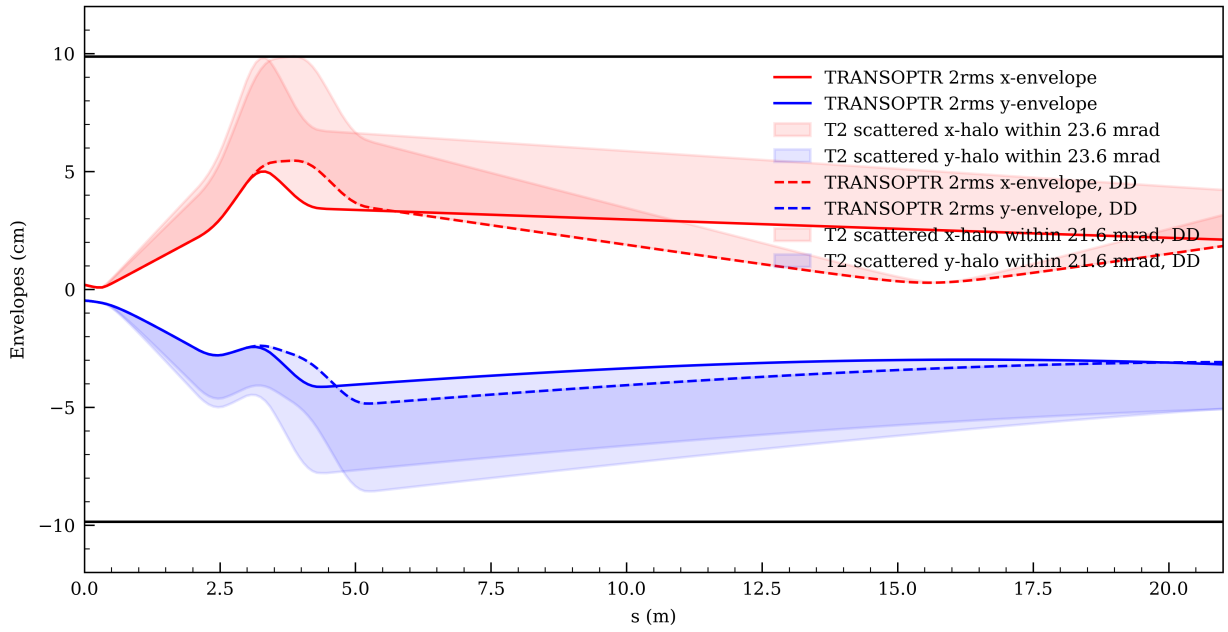

Figure 4: Halo from T2 scattering. For the original triplet optics, shown by the solid lines, halos with scattering angles larger than 23.6 mrad will eventually be lost along the beamline. For the DD (double doublet) optics, shown by the dashed lines, the critical scattering angle is 21.6 mrad. In an ideal collimator designed to stop all particles that hit it, the inner aperture should match the halo envelope. A conical shape with a cone angle of 20 mrad is sufficient to achieve this for both optic models.

4 Collimator Material Selection

The choice of material for the collimator is a balance between stopping power, thermal management, and secondary particle production. Key considerations include: High-Z materials like tungsten or lead offer excellent stopping power and are ideal for stopping the protons. Graphite may be used as a low-Z material in the first stage collimator to reduce secondary particle production before final collimation by higher-Z material. Copper or Beryllium are options for areas where good thermal conductivity is necessary to prevent overheating from energy deposition.

The property of the commonly used material for collimator is summarized in table 3. The data are found from the Particle Data Group website [7], where most of the data is measured experimentally. The average path length traveled by a charged particle as it slows down to rest, calculated in the continuous-slowing-down approximation (CSDA). In this approximation, the rate of energy loss at every point along the track is assumed to be equal to the total stopping power. The CSDA range in the table is from US. National Institute of Standard and Technology.[8]

Table 2: Collimator Material Selection. CSDA range is calculated with 454 MeV proton beam.

Material	**Density** (g/cm^3)	**CSDA range** (g/cm^2)	**Thermal Con.** (W/m·K)	**Melting Point** (°C)	**Radiation Length** (g/cm^2)
Tungsten (W)	19.3	191	173	3422	6.76
Lead (Pb)	11.4	198	35	327	6.37
Copper (Cu)	8.96	148	401	1085	12.86
Graphite (C)	1.70	113	110	3652	42.70
Beryllium (Be)	1.85	124	200	1287	65.19

For the first stage collimation of the the primary proton beam, we require smaller slits scattering and good thermal conductivity. Copper and Beryllium are good. To fully stop the 454 MeV proton beam halo after T2 target, a 17 cm copper or 67 cm Beryllium is sufficient. Considering the tight space in the collimation section, copper is preferable.

For the second stage collimation of the scattered proton beam from the first stage collimator. A high-Z materal would be better. In this note, we optimize the geometry using Copper.

5 Geometric Configuration

The existing design incorporates two separate collimators, referred to as COLA and COLB in this design note. The geometry of COLB was highly optimized by Templeton [9] for the 10 cm Be target. However, Templeton raised concerns about the difficulty of modifying COLB, stating, "There is some uncertainty in the reliability of the collimator optimization calculations. Col B can only be accessed at great inconvenience and even then modifications would be difficult. Thus, the option of inserting a liner in the easily assessed Col A may prove to be essential should these calculations turn out to be less accurate than we expect." Looking at the present collimator section, COLA has been inserted in the removable medical blocker, that proves the geometry of COLA provides a good backup during commissioning, allowing for adjustments if COLB does not perform as expected. The sketch of the existing collimator geometry is shown in Fig. 5. The parameters could be found in the requirements specification[10].

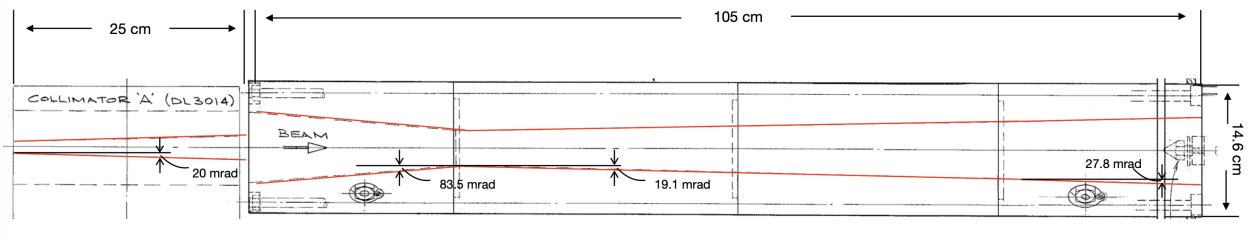

Figure 5: Geometry model of current collimator A and collimator B.

The new design features two stages of collimation to optimize spill control and transmission efficiency. The primary collimator, COL A, is positioned immediately downstream of the T2 target to collimate the halo generated by the target. Following a drift space, the secondary collimator, COL B, intercepts both the scattered halo from COL A and any primary halo that escapes the first collimator.

5.1 Primary Collimator

As shown by the beam halo envelopes in Fig. 18. , the inner geometry of the collimator must follow the halo envelope to effectively collimate the scattering halo. To further optimize the performance with considering the scattering caused by collimators, we performed a parameter scan around the theoretical geometry to identify the optimal design parameters.

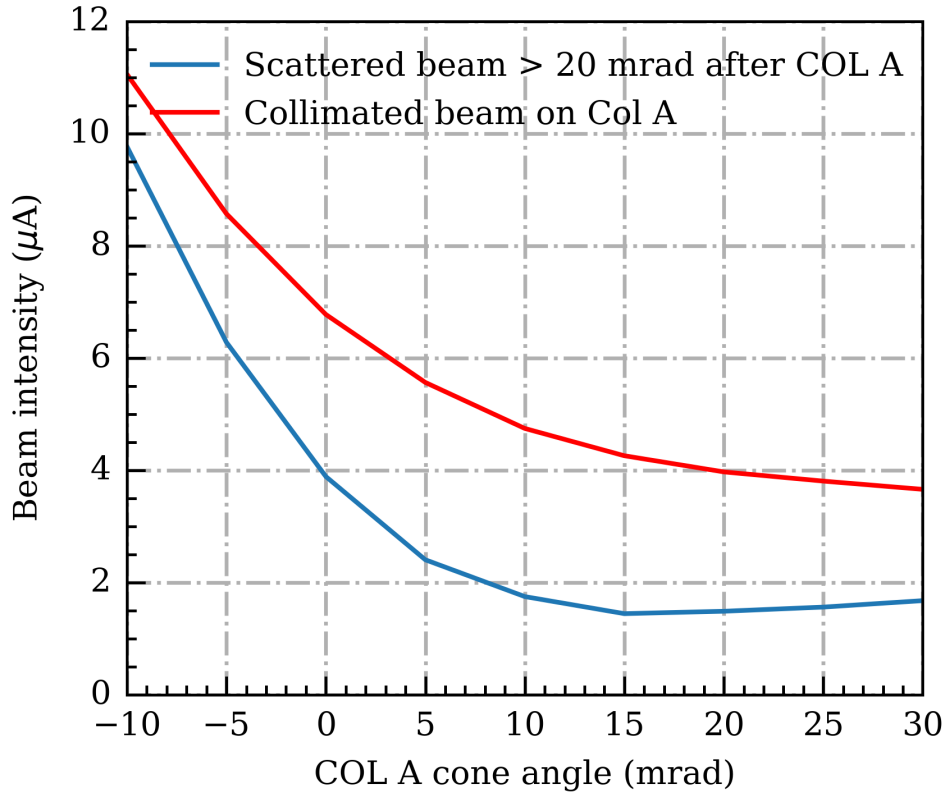

Figure 6: COL A cone angle optimization. Beam halo particles with scattering angles greater than 20 mrad will eventually be lost along the beamline if not intercepted by the collimator. To minimize spills downstream of COL A, the optimal cone angle is determined to be between 15 and 20 mrad, as shown by the blue line. The increase in spills slows significantly beyond 15 mrad. Therefore, the existing design with a 20 mrad cone angle is adequate.

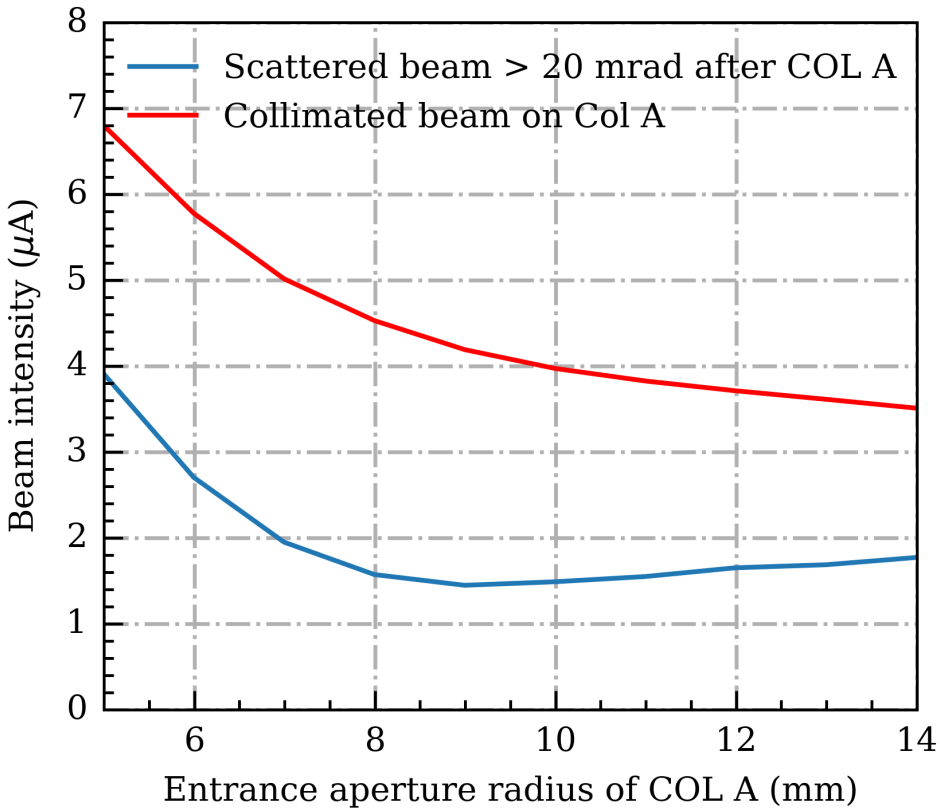

Figure 7: COL A aperture optimization. Similar to the cone angle optimization, the optimal aperture for COL A is found to be between 9 mm and 10 mm. The existing design with a 10 mm aperture is adequate.

5.2 Secondary Collimator

To further capture residual halo particles and those scattered by COL A, a secondary collimator, COL B, is mandatory to minimize downstream spills. The optimal geometric parameters for COL B are determined using the same method as applied in the COL A design, involving a parameter scan around the theoretical values suggested by the halo envelope.

The G4 model of the simulation is shown in Fig. 8. The collimator sections are embedded within the T2 monument. The monument model is extracted from Syd Kreitzman's target station model [11]. The available space for the collimators could be extended beyond the monument, reaching up to the front of the triplet.

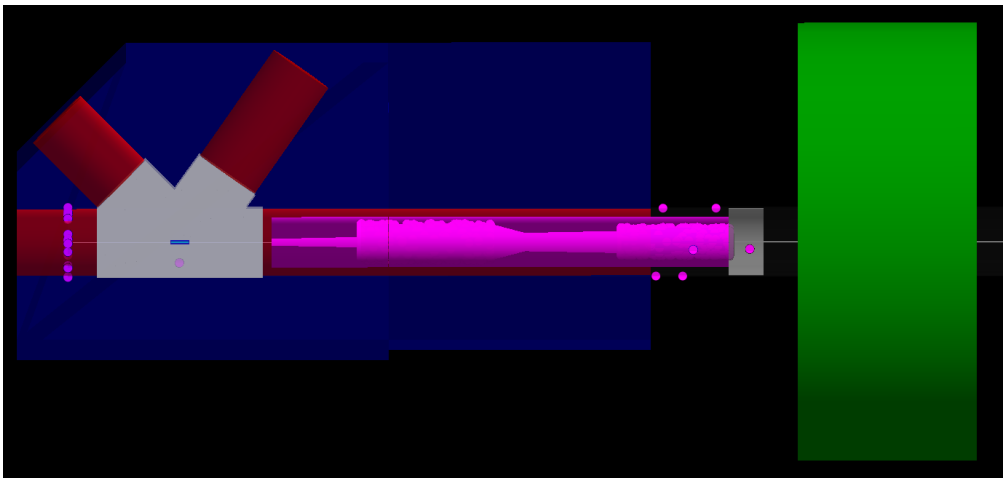

Figure 8: G4 model of the collimator section. the blue block represents the T2 monument, while the green cylinder corresponds to Q14. The collimator section is designed to fit within the magenta cylinder.

6 Collimator Geometry Optimization

The geometric parameters, including length, aperture, cone angle, collimator location, and tapered section, have been optimized. The details of this optimization are presented in this section. The resulting optimal geometry for the collimators is illustrated in Fig. 15, showing a significantly shorter COL B compared to the original design.

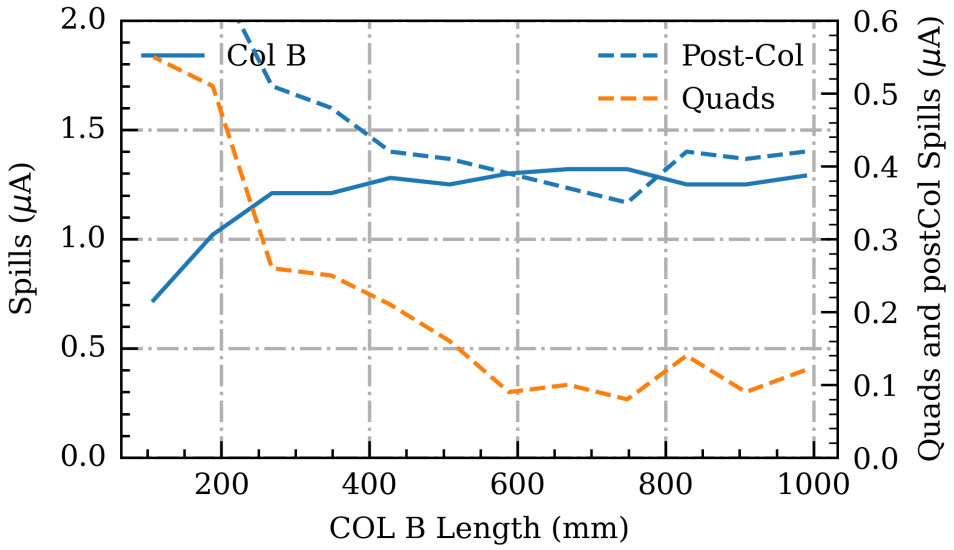

Figure 9: COL B length. In the ideal case, without accounting for scattering from the collimator, a 17 cm collimator with a cone aperture matching the halo envelope size and a cone angle of 20 mrad should effectively collimate all halos. When scattering is considered, a longer collimator is required. We begin with a collimator aperture as defined in the ideal case and a maximum length constrained by the available space, then gradually shorten the collimator by removing sections from the entry end. It was observed that the first 400 mm of the collimator does not impact downstream spills as shown by the dashed lines or beam loss on the collimator shown by the solid line. This is because a drift space is necessary for scattered particles to deviate sufficiently from the beam axis and get intercepted by the collimator.

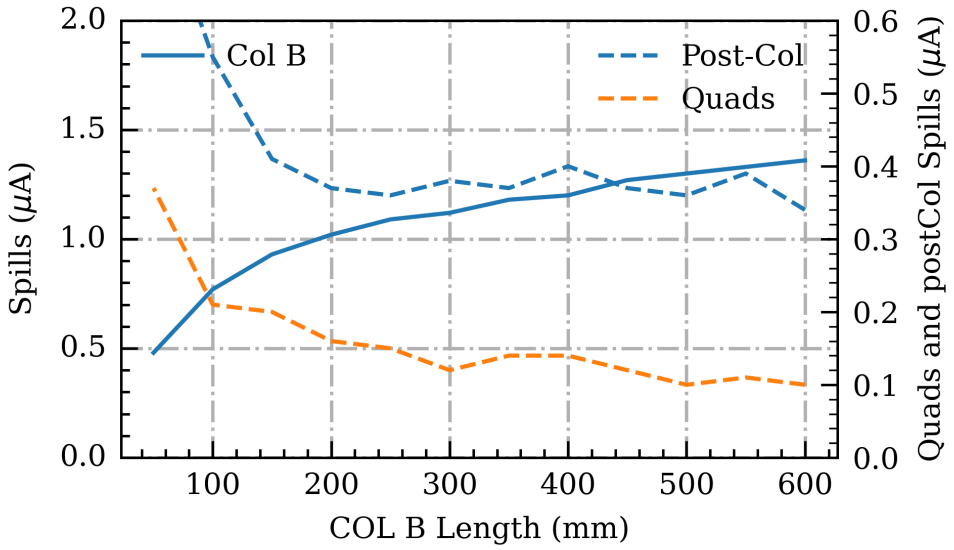

Figure 10: COL B length. Fig. 9 demonstrates the redundancy in the entry end of the collimator. By starting with a collimator shortened by 400 mm from the entry, additional reductions were systematically made from the exit end. The results confirm that redundancy exists at both ends of the collimator. A 300 mm length was identified as optimal when balancing transmission efficiency and minimizing downstream spills. However, to enable the introduction of a tapered entry for further optimization, a slightly longer length of 380 mm was chosen. This compromise ensures both optimal performance and the flexibility needed for further refinement.

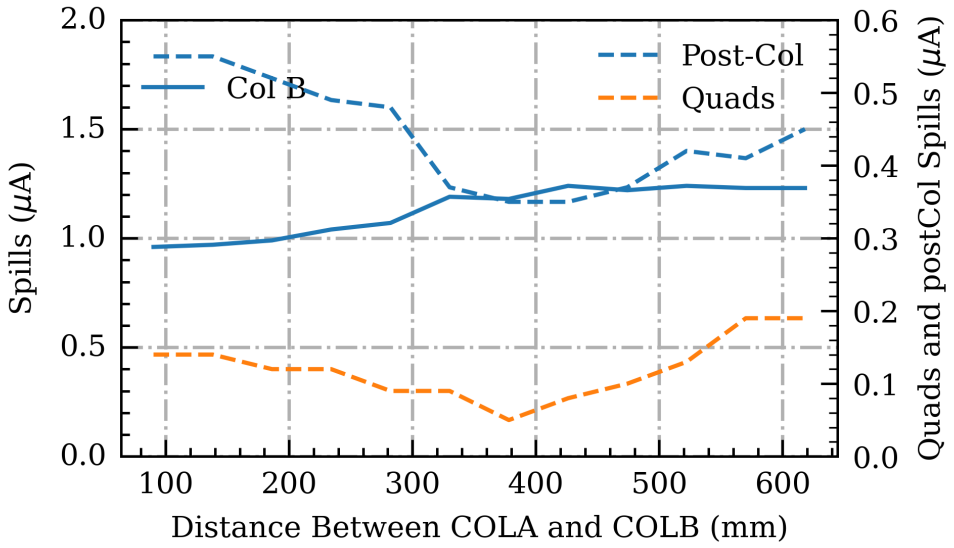

Figure 11: COL B position. Positioning COL B further away from COL A should improve collimation efficiency, as scattered particles move farther from the beam axis with increasing longitudinal distance. However, the presence of the monument, which can also capture scattered particles from the collimator, leads to an increase in downstream spills when the collimator is positioned too close to or extends beyond the exit of the monument. The optimal distance between COL A and B is around 380 mm.

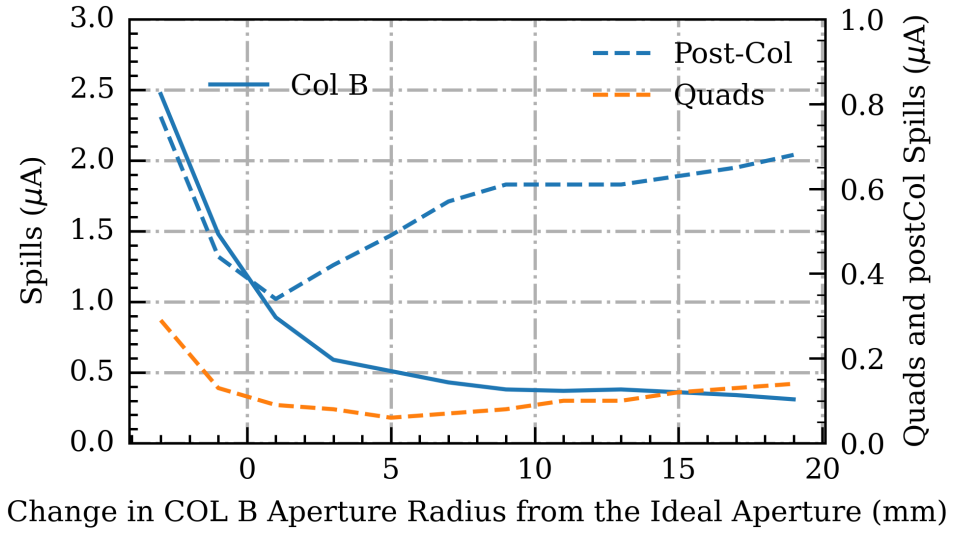

Figure 12: COL B aperture optimization. With the cone angle of the aperture fixed, smaller aperture collimate out more halo on the collimator but also generates more scattering. Balancing these effects, to minimize the spills on the triplet and in the Post-Col section, the optimal aperture for the collimator is determined to be 2 mm larger than the ideal aperture suggested by the halo envelope.

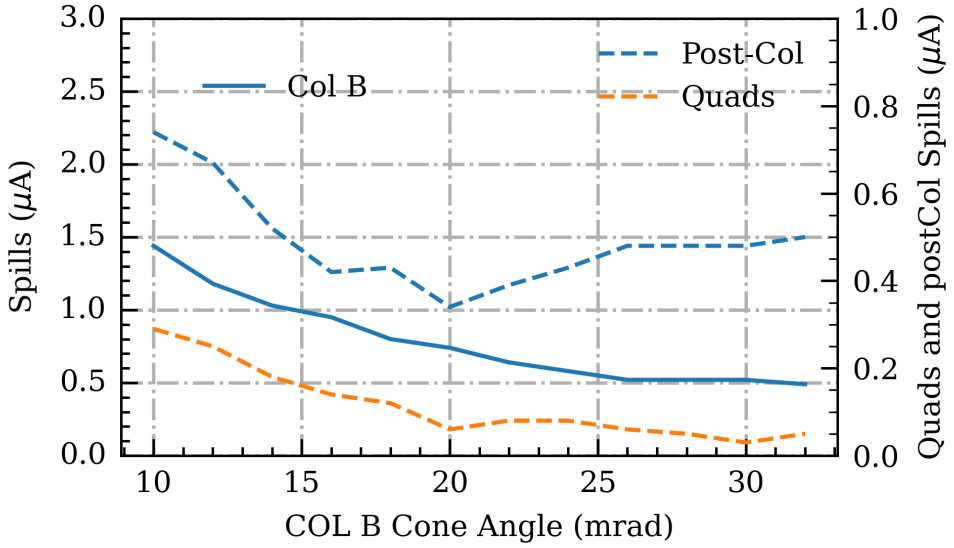

Figure 13: COL B cone angle optimization. The ideal cone angle suggested by the envelope model is 20 mrad, and the G4 simulation gives a similar optimal value. Therefore, the same 20 mrad cone angle used for COL A is also adopted for COL B.

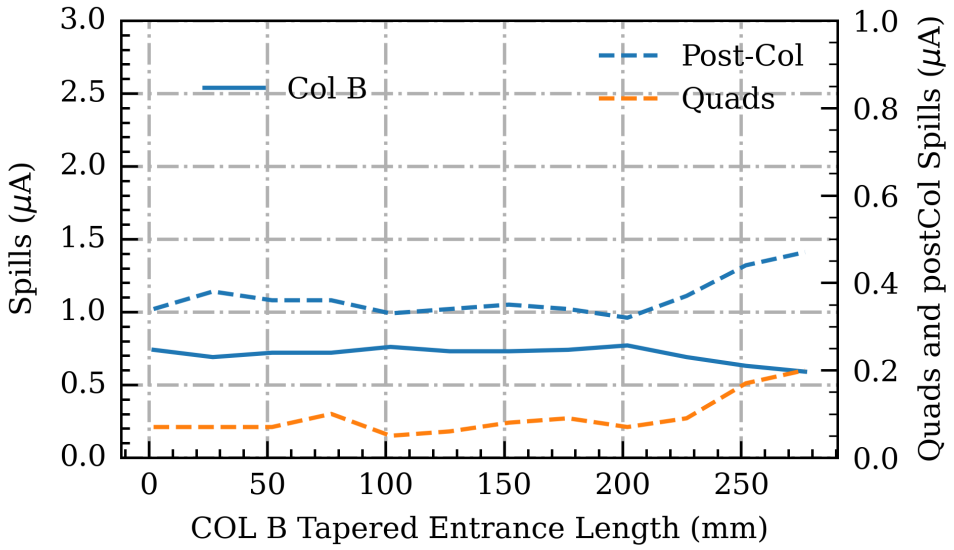

Figure 14: Tapered entrance. A tapered entrance could further reduce the scattering particles from COL B, with a 100 mm tapered section, the spills on the quads are reduced by another 20 nA. More importantly, the tapered entrance helps distribute the heat more evenly across the collimator.

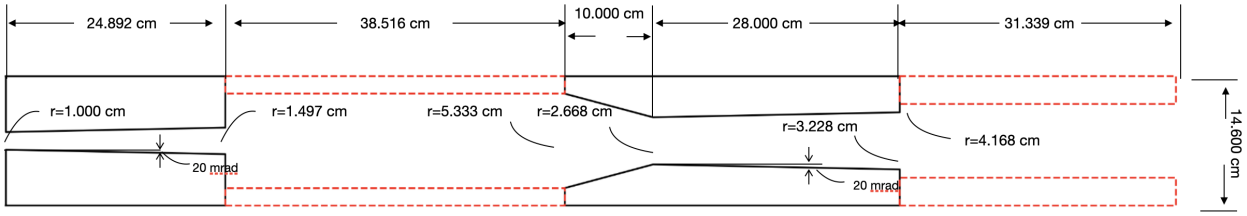

Figure 15: Optimal collimator geometry. The solid black line represents the geometry of COL A and COL B, while the dashed red line indicates the allowable area for installing supporting structures and cooling systems without impacting collimation performance.

7 Collimator Performance

For the primary collimator (COL A), the existing design is already very close to the optimal configuration, so no changes are needed in the new design. In contrast, the secondary collimator (COL B) has significant modifications. The performance of the new collimator is shown in Fig. 16, and a comparison with the original design is summarized in Table 2.

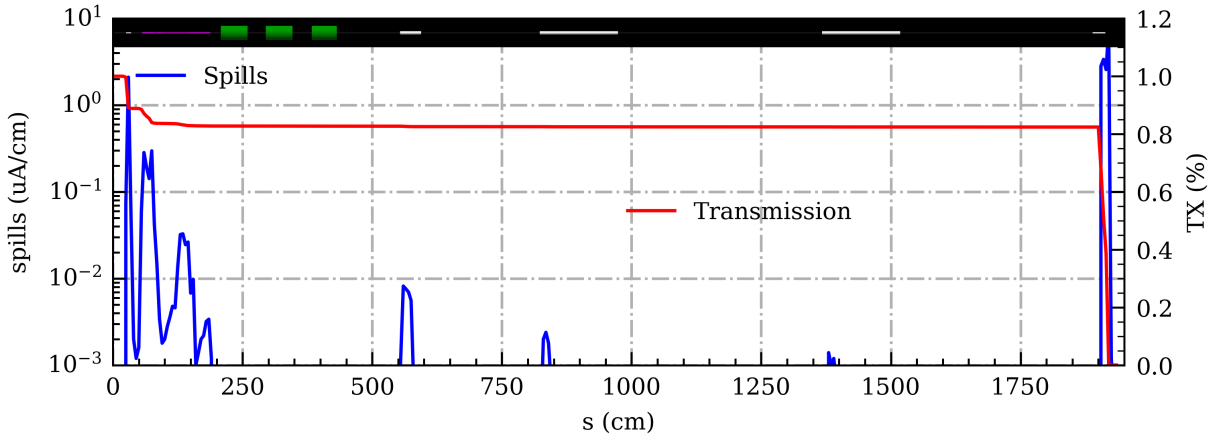

Figure 16: Beam spills and transmission with the new design. Comparing with the original design shown in Fig. 3, the spills in the triplet section and scraper boxes are lower.

Table 3: Performance comparison.

	Spills in COL B setion (μA)	**Spills on quads (μA)**	**Spills Post-Collimator (μA)**
Original	1.63	0.09	0.43
Optimized	0.78	0.05	0.33

8 Misalignment Tolerance

In this section, we systematically introduce misalignments in the collimator's positioning and analyze their impact on spills to determine the tolerance to misalignment. Simulations indicate that a transverse misalignment of several millimeters is tolerable with respect to the increase in spills on the triplet. A typical centering error of the beam on T2 is within several millimeters (maximum 0.3 inch vertically) and less than 10 mrad [12], with a misalignment of COL B relative to the centerline T2 of similar magnitude. Under these conditions, the heat load on COL B could increase to approximately 667 W.

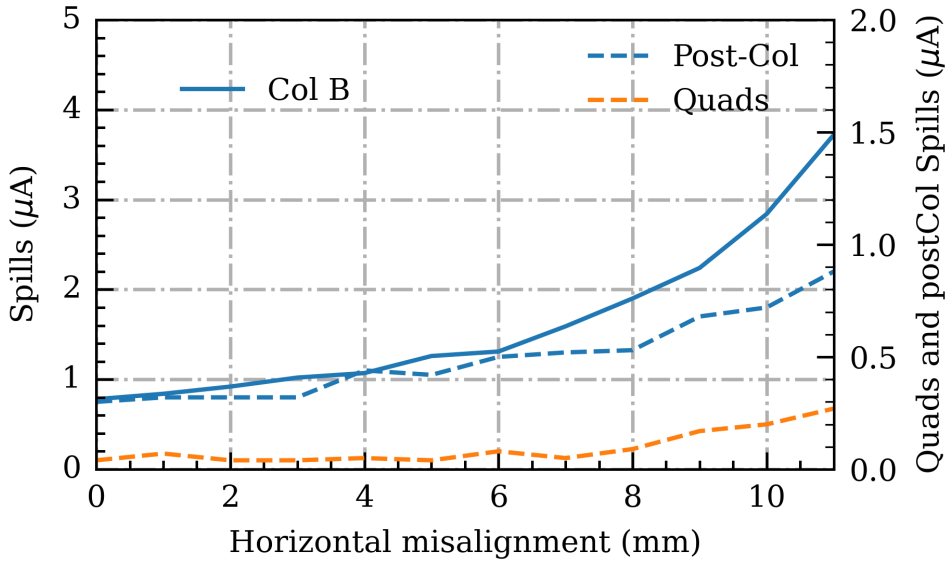

Figure 17: Horizontal misalignment. As the horizontal misalignment increases, the spills generally increase for all three components (Col B, Post-Col, and Quads). As the misalignment increases, the spills rise more steeply. A 9 mm misalignment doubles the spills.

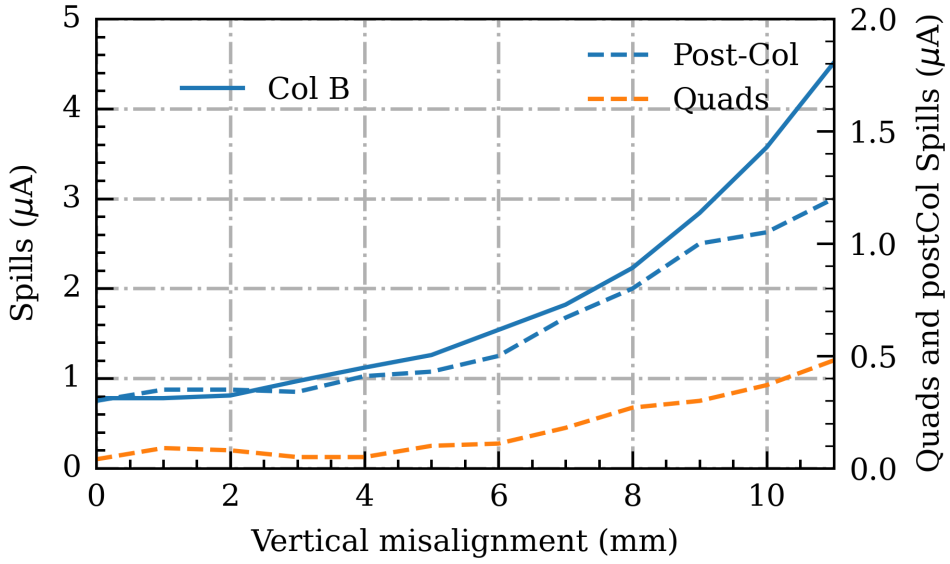

Figure 18: The trend of spill increase with vertical misalignment is similar to that of horizontal misalignment, but the sensitivity is greater. A 7 mm vertical misalignment doubles the spills.

9 Conclusions

The G4 simulation model was developed to optimize the collimator design and has been validated against the TRANSOPTR model and experimental data from production runs.

In the original design, COL B was implemented as a single long collimator optimized for spills and transmission, with a replaceable COL A liner included as a backup plan to account for computational uncertainties. However, operational experience indicated that the COL A liner is essential to control downstream spills.

Our optimization incorporates a two-stage collimation strategy, optimizing both COL A and COL B together. The results show that the existing COL A liner is adequate, while COL B has significant redundancy. The optimized COL B design is considerably shorter, achieving a 44 % reduction in spills on downstream quadrupoles and a 23 % reduction in total downstream spills.

A sensitivity study on misalignment revealed that the tolerance for horizontal and vertical misalignments of COL B is on the order of several millimeters. These tolerances are primarily constrained by the downstream spill levels and the cooling capacity of COL B.

References

[1] L. Zhang, BL1A Study Using G4Beamline and TRANSOPTR: Calibrate the Beam Parameters on the Target, Tech. Rep. TRI-BN-19-03, TRIUMF (2020).

[2] L. Zhang, G4beamline simulation of Collimation and Spills between T2 and TNF in BL1A , Tech. Rep. TRI-BN-23-21, TRIUMF (2023).

[3] E. W. Blackmore, A. Dowling, R. Ruegg, M. Stenning, Operating experience with meson production targets at triumf, in: Proceedings of the 2005 Particle Accelerator Conference, IEEE, 2005, pp. 1919–1921.

[4] F. Jones, BL1A Simulation Model in G4Beamline, Tech. Rep. TRI-BN-19-03, TRIUMF (2019).

[5] Y.-N. Rao, R. Baartman, Current Status of Beamline 1A Optics, Tech. Rep. TRI-BN-22-05, TRIUMF (2022).

[6] Y.-N. Rao, Improved Beam Line 1A (BL1A) Optics, Tech. Rep. TRI-DN-22-09, TRIUMF (2022).

[7] [link].
URL `http://pdg.lbl.gov/2009/AtomicNuclearProperties/`

[8] [link].
URL `https://physics.nist.gov/PhysRefData/Star/Text/PSTAR.html`

[9] T. Templeton, A. Arrott, P. Reeve, Spill Calculations and Ceam Collimation in Beam Line 1a between T1 and TNF, Tech. Rep. TRI-BN-77-18, TRIUMF (1977).

[10] R. Brar, Discussions to Finalize the New and Optimized Collimator 1A, PRJ-575 T2 Leak Issue, Tech. Rep. Document-243914, TRIUMF (2024).

[11] S. Kreitzman, Private communication, personal communication (2024).

[12] Y.-N. Rao, BL1A T2 Issue, Tech. Rep. TRI-BN-17-23, TRIUMF (2017).